Folia Neuropathologica

The effect of propofol on astro- and microglial reactivity in the course of experimental intracerebral haemorrhage in rats

Zbigniew Karwacki[1], Przemysław Kowiański[2], Jerzy Dziewiatkowski[2], Beata Domaradzka-Pytel[2], Beata Ludkiewicz[2], Sławomir Wójcik[2], Olgierd Narkiewicz[2], Janusz Moryś[2]

[1]Department of Neuroanaesthesiology, Medical University of Gdańsk, Poland; [2]Department of Anatomy and Neurobiology, Medical University of Gdańsk, Poland

Folia Neuropathol 2006; 44 (1): 50-58

Abstract

The glial cells play an important role in pathophysiology of the intracerebral haemorrhage (ICH). Thus the attempt at evaluating the possible influence of the propofol on the reactivity of astro- and microglial cells in the course of ICH was performed.

50 rats were divided into two groups depending on the applied anaesthesia. All animals were generally anaesthetized with fentanyl, dehydrobenzperidol and midazolam. No additional agents were given to the animals of the control group (group I). In the experimental group (group II), the animals received additionally intraperitoneally propofol in a dose of 50 mg/kg every thirty minutes. ICH was produced through infusion of the blood into the striatum. The astrocytic and microglial cells population was assessed on the 1, 3, 7, 14 and 21 days after producing a haematoma using antibodies anti-GFAP and OX42. The stereological analysis was applied to estimate the numerical density of immunoreactive cells and the distribution of their types.

On the 14th and 21st days of observation the density of GFAP-immunoreactivity (ir) cells was significantly higher in group II than that in group I. There were no differences in percentage distribution of GFAP-ir astrocytes between group I and group II. On the 3rd, 14th and 21st days of observation the density of OX42-ir cells was higher in group II in comparison with group I. For the 7th, and 21st days of survival the percentage of the ameboid form of OX42-ir cells was significantly lower in group I than that in group II.

The administration of propofol during anaesthesia in the animals with ICH has evoked an increase of the activation of the astro- and microglial cells.

Key words: *propofol, astrocyte, microglia, intracerebral haemorrhage, rat.*

Introduction

Intracerebral haemorrhage (ICH) is a common and often fatal stroke subtype that leads to a severe neurological damage in survivors with no effective treatment. The current strategy of management of ICH remains controversial. There is no clear indication from the literature of the optimal treatment of ICH surgical or otherwise [5]. Regardless of the applied method, the main goal of treatment of ICH should include control of systemic hypertension and prevention or treatment of the

Communicating author:

Zbigniew Karwacki, MD PhD, Department of Neuroanaesthesiology, Medical University of Gdańsk, 7 Dębinki St., 80-211 Gdańsk, tel. +48 58 349 23 35, fax +48 58 349 14 21, e-mail: zkarw@amg.gda.pl

elevated intracranial pressure [23]. Most authors suggest removing of the cerebellar and superficial lobar haematomas [6]. Different methods of surgical treatment of ICH, for instance, open craniotomy [6], the use of endoscopy [3] or a stereotactic injection of thrombolytic agents for liquifying clot and removal [18] have been proposed.

Developing an effective method of treatment means an improved understanding of the pathophysiology of ICH [13]. Recently published investigations direct attention to perihaematomal region as a potential target for therapeutic intervention in the ICH patient [1,7,27,31]. The mechanical injury caused by extravasation of blood leading to reduction of the cerebral blood flow [20,21], inflammatory reaction [8,17] breakdown of hemoglobin [11,37] and complement cascade activation [10,36] have all been implicated as mediators of tissue injury. In these processes the astroglial and microglial cells play an important role. Even minor pathology induces morphological transformation of these cells from resting into activated forms. Activated astrocytic cells synthesize and secrete tumor necrosis factor-alfa, interleukin-1-beta and interleukin-6 [8,20,37]. Activated astrocytes play an important role in formatting the glial scar that is the result of the repair response of the glial [8,20,17]. Ameboid forms of microglial cells are able to migrate [28] and capable of proliferating and phagocyting [27]. Released form activated microglia tumor necrosis factor-alfa and interleukin-1-beta are responsible for damage of the blood-brain-barrier in the course of ICH [9]. Literature concerning the reaction of astro- and microglial cells in the course of ICH is poorly represented [7,14,15].

Propofol remains a commonly used agent for providing intraoperative anaesthesia as well as sedation in the patient treated in the intensive care unit. Many laboratory and clinical investigations confirm the favorable influence of propofol on intracranial homeostasis [30]. Effects on the cerebral blood flow [16,34], cerebral metabolic rate for oxygen [33] intracranial pressure [22] and neuroprotective property [26,39] give sufficient grounds for recommendation of propofol for neurosurgical procedures.

The proposal of the present study was to investigate whether propofol attenuates reactivity of astroglial and microglial cells in the course of experimental intracerebral haemorrhage in rats.

Table I. Physiological parameters in groups I and II in the middle stage of production of intracerebral haematoma*

Parameter	Group I	Group II
body weight (g)	300.5±14.3	309.2±13.9
hemoglobin (g dL^{-1})	12.73±1.11	11.3±1.7
glucose (mmol.l)	8.11±0.71	7.97±0.97
temperature (°C)	37.3±0.1	37.2±0.1
$ETCO_2$ (kPa)	5.24±0.05	5.26±0.04
SaO_2 (%)	96.7±0.5	96.5±0.9
CPP (mmHg)	89.2±4.9	88.9±5.1

**Data are presented as mean ± standard deviation*

Material and methods

50 adult rats (weight 275-350 g; Table I) were used in the study. Animal care and treatment guidelines outlined by the European Community Council Directive of 24 November 1986 (86/609/EEC), as well as the local ethical committee were followed. Animals were divided into two groups depending on the applied anaesthesia. In all the groups, the animals were generally anaesthetized with fentanyl (Fentanyl, Polfa-Warszawa, Poland) with a dose of 0.02 $mg.kg^{-1}$, dehydrobenzperidol (Droperidol, G .Richter; Hungary) with a dose of 0.75 $mg.kg^{-1}$ administered intraperitoneally and midazolam maleate (Dormicum, Roche; Switzerland) with a dose of 0.3 $mg.kg^{-1}$ given intramuscularly every half hour. No additional agents were given to the animals of group I. In group II the animals received additionally intraperitoneally propofol (Diprivan, AstraZeneca; United Kingdom) with a dose of 50 mg/kg every thirty minutes. Each group was divided into five subgroups (five animals in each subgroup) depending on the length of the survival period: 1, 3, 7, 14, 21 days.

After insertion of the intubation tube, the rats were mechanically ventilated with the Small Animal Ventilator SAR 830/p (CWE, Inc. USA), using a mixture of air and oxygen (FiO_2 = 0.5). Parameters of ventilation were adjusted to keep the end-tidal concentration of CO_2 ($ETCO_2$) constant between 5.19 and 5.45 kPa, and O_2 saturation of the hemoglobin (SaO_2) above 95%. $ETCO_2$ was monitored with the carbon dioxide analyzer Capstar 100 (CWE, Inc. USA). Continuous monitoring of the SaO_2 was performed with pulse oximeter monitor

(Novametix; USA) connected with a sensor placed across the animal's hind foot.

Both the femoral artery and vein were cannulated for continuous mean arterial blood pressure monitoring (MAP), blood sampling for biochemical analysis as well as fluid infusion. MAP was monitored with the direct blood pressure monitor (Stoelting; USA). Maintenance fluids (0.9% NaCl) was administered at the rate of 2.5 $ml.kg^{-1}.h^{-1}$. Body temperature was maintained at 37.0°C (Table I) using a rectal thermometer and a feedback-controlled heating pad (EST, Stoelting; USA).

The animal was fixed in a stereotaxic frame and than MicroSensor ICP Transducer (Codman Johnson & Johnson Medical Ltd, USA) was inserted epidurally in the parietal region through a separate trepanation hole. For continuous measurement of ICP, the transducer was connected to the Neuro Monitor Interface Control Unit (Codman, Johnson & Johnson Medical Ltd. USA) and a Monitoring System 8000 (Simonsen & Weell; Denmark). A hole was drilled in the frontal bone on the opposite side to the ICP monitoring. After introducing the needle into the striatum (stereotaxic coordinates: B=1.2 mm; L=2.5 mm; H=5.5 mm), 100 µl of autologous blood was injected for 5 minutes and the needle was left in place for another 4 minutes, than it was slowly withdrawn and the skull was sealed.

During the production of haematoma, the plasma levels of glucose and hemoglobin (Table I), were measured using the B-Hemoglobin and B-Glucose Analyzer (HEMOCUE AB, Sweden). Comparability of the physiological condition during the experiments were maintained using continuous monitoring of $ETCO_2$, SaO_2, and cerebral perfusion pressure (CPP). CPP was calculated from the difference between MAP and ICP. Appropriate results are given in table I. After the experiment the rats were allowed to awake under control of $ETCO_2$ and SaO_2. The intubation tube was removed if spontaneous breathing of animals was sufficient (values of $ETCO_2$ below 5.32 kPa, and SaO_2 above 95%).

Immunohistochemistry

The animals were deeply anesthetized with lethal doses of thiopental sodium (Thiopental, Biochemie GmbH, Austria) with the dose of 50 $mg.kg^{-1}$, then transcardially perfused with 0.9% solution of NaCl, followed by a 4% paraformaldehyde solution in 0.1M phosphate buffer (pH 7.4). The brains were postfixed in 4% paraformaldehyde fixative for 3-4 hours, and then were kept in 0.1 M phosphate buffer containing 15% sucrose (overnight at 4°C) and 30% sucrose (until sunk). Coronal 50-µm-thick serial sections of the brain (five from each animal) were cut with JUNG 1800 cryostat (Leica, Germany). Free floating sections were blocked with 3% NGS containing 0.4% Triton X-100 for 1 hour and then were incubated with the monoclonal antibody (mAb) OX42 recognizing the complement type -3 receptor (CR3/CD11b) (mouse, dilution 1:50, MCA275G, Serotec, Cambrige, UK) and with the primary antibodies anti- GFAP (dilution: 1:250, DAKO, Denmark). After multiple rinses in PBS, the sections were incubated (2-3 hours, room temperature) with the secondary antibody conjugated with Cy3 (dilution: 1:500, Jackson Immuno Research, USA) or FITC (dilution: 1:50, Jackson Immuno Research, USA). The chosen set of brain sections of both the experimental as well as control groups underwent negative control with omission of the primary antibody.

Qualitative assessment of glial activation

Structures as well as the localization and morphology of the haematoma were assessed on the sections stained with cresyl violet using Labophot (Nikon, Japan) referring to the stereotactic atlas of the rat brain.

Immunohistochemically labeled sections were analyzed using the fluorescent microscope BX-51 (Olympus, Japan), and confocal laser scanning µ-Radiance head (Bio-Rad, United Kingdom) mounted on Eclipse E600 microscope (Nikon, Japan). FITC and Cy^3 were excited by a monochromatic beam of 488 nm and 514 nm of length, respectively. 3D stacks of optical confocal scans were obtained by the usage of high quality 20x and 60x oil lenses and optimal iris in LaserSharp 2000 (Bio-Rad, United Kingdom).

The distribution of immunopositive cells and their morphological type were assessed.

Quantitative assessment of microroglial activation

Intensity of glial reaction was quantified by the number of labeled cells per unit area using C.A.S.T. Grid stereological system (Olympus; Denmark). The

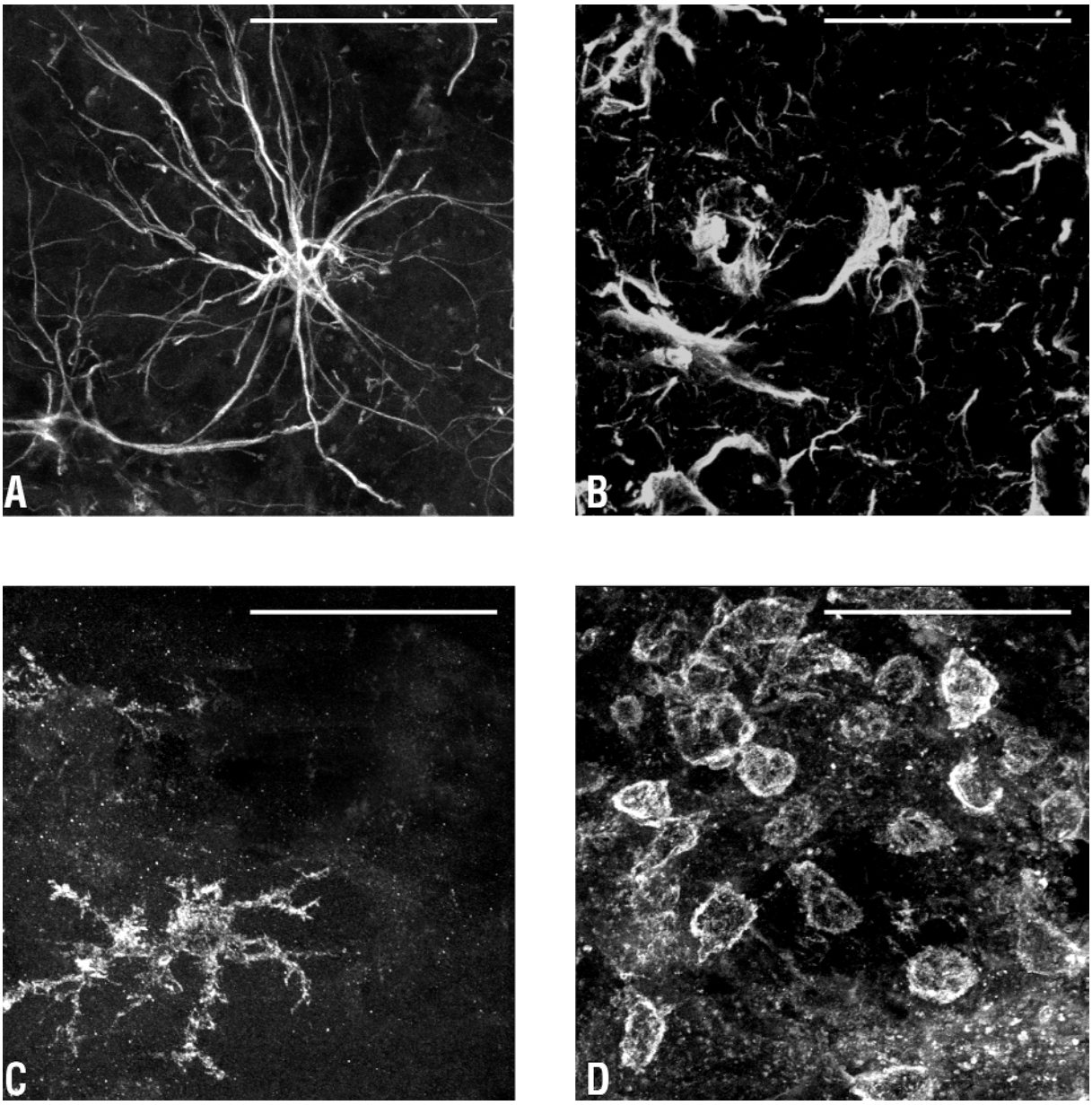

Fig. 1. Types of astroglial and microglial cells: resting form of astrocyte (**A**), activated astrocyte (**B**), resting form of microglia (**C**), ameboid form of activated microglia (**D**). Staining A-B-GFAP, C-D-OX42. Magnification bar=50 µm

reference area bordered by the ventricle, corpus callosum, external capsule and the level of rhinal sulcus with the exclusion of the haematoma region were marked and measured under the small magnification. Cells were counted in test frames (of area equal to 0.2765 mm^2) chosen in a systematic random fashion. As a minimum one third of the reference area was assessed. On the basis of their morphology astroglial and microglial cells were classified into resting (Fig. 1A, C) and activated (Fig. 1B) or ameboid (Fig. 1D) types. The data were then transferred to the spreadsheet; the number of cells per unit area was calculated. Finally, the mean value of the numerical density of glial cells as well as the percentage distribution of their types in each case were estimated.

The statistical analysis was done by means of *Statistica v. 6.0* (Statsoft; USA) and *GraphPad Instat* (Graph Pad Inc.; USA). The significance of differences of values of body weight, glucose, hemoglobin, temperature, $ETCO_2$, SaO_2, as well as CPP between groups I and II were assessed by the Mann-Whitney test. The influence of the anaesthetic agent and period of survival on the numerical density and percentage distribution of glial cells were tested using the analysis of variance followed by the LSD test for the planned study of differences between groups and subgroups. 95% confidence intervals for the differences between means were calculated.

Results in the tables and graphs are expressed either as mean ± standard deviation or as mean ± standard error of mean (SE); used parameter is indicated. A p-value less than 0.05 was considered statistically significant.

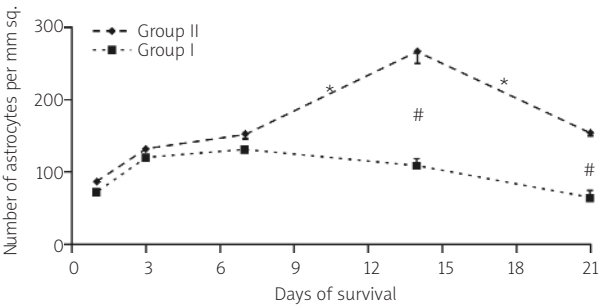

Fig. 2. The number of GFAP-ir cells (per unit area) within the reference area on 1, 3, 7, 14 and 21 days after haematoma occurrence in groups I and II. Data are presented as mean±standard error. Significant differences between survival groups are marked by asterisks while those between groups I and II -by hashes

Results

In group II significant differences in the density of GFAP-ir astrocytes were observed between the 7th and 14th and 14th and 21st days of survival (Fig. 2, Tab. II). On the fourteenth and twenty first days after production of haematoma statistically significant differences in the numerical density of GFAP-ir astrocytic cells between groups I and II were noted (Fig. 2, Tab. II). In group I there was an increase in per cent distribution of activated GFAP-ir cells that remained up till the end of the observation (Fig. 3, Tab. II). In group II there was an increase in per cent distribution of activated GFAP-ir cells between the 1st and 3rd that decreased between the 3rd and 7th and than again increased between the 7th and 14th days after production of haematoma (Fig. 3, Tab. II).

In group I there was an increase of density of OX42-ir microglia only between the 3rd and 7th observation days whereas in group II an increase of the number of OX42-ir per mm sq. was found between the 7th and 14th observation days, and then a decrease between the 14th and 21st days after production of haematoma (Fig. 4, Tab. III) On the third, fourteen and twenty first observation days differences in the numerical density of OX42-ir microglia between groups I and II was observed (Fig. 4, Tab. III).

Table II. Significant differences between the means along with 95% confidence intervals (CI) and p-value of the LSD test (p) for analyzed parameters of GFAP-ir astrocyte

Parameter	Groups	Survival day	Difference	Lower 95% CI	Upper 95% CI	p
numerical density of astroglia	group II	7 vs 14	-113.132	-168.392	-57.872	0.000184
numerical density of astroglia	group II	14 vs 21	111.449	52.09	170.808	0.000507
numerical density of astroglia	group II vs group I	14	158.31	103.05	213.57	0.000001
numerical density of astroglia	group II vs group I	21	91.211	22.669	159.753	0.010453
per cent of activated form	group II	1 vs 3	-88.8313	-95.0398	-82.6229	0.00012
per cent of activated form	group II	3 vs 7	10.4696	3.6686	17.2706	0.003479
per cent of activated form	group II	7 vs 14	-7.461	-13.2408	-1.6813	0.012779
per cent of activated form	group I	1 vs 3	-85.575	-94.3551	-76.7949	0.00031

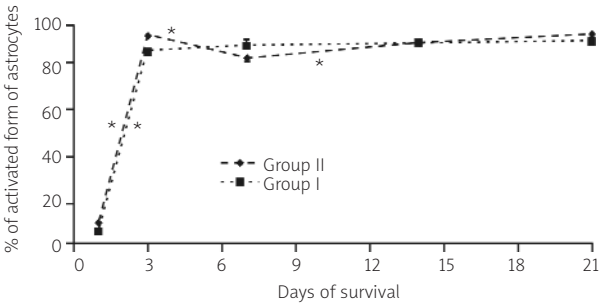

Fig. 3. Per cent of the activated form of GFAP-ir cells within the reference area 1, 3, 7, 14 and 21 days after haematoma occurrence in groups I and II. Data are presented as mean±standard error. Significant differences between survival groups are marked by asterisks while those between groups I and II -by hashes

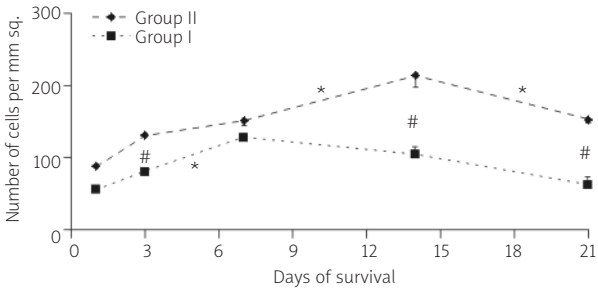

Fig. 4. The number of OX42-ir cells (per unit area) within the reference area on 1, 3, 7, 14 and 21 days after haematoma occurrence in groups I and II. Data are presented as mean±standard error. Significant differences between survival groups are marked by asterisks while between groups I and II -by hashes

Table III. Significant differences between the means along with 95% confidence intervals (CI) and p-value of the LSD test (p) for analyzed parameters of OX-42-ir microglia

Parameter	Groups	Survival day	Difference	Lower 95% CI	Upper 95% CI	p
numerical density of microglia	group I	3 vs 7	-48	-94.301	-1.699	0.042602
numerical density of microglia	group II	7 vs 14	-60.819	-102.232	-19.406	0.005269
numerical density of microglia	group II	14 vs 21	59.136	15.211	103.061	0.009859
numerical density of microglia	group I vs group II	3	-52.018	-98.32	-5.717	0.028825
numerical density of microglia	group I vs group II	14	-108.397	-149.81	-66.984	0.000007
numerical density of microglia	group I vs group II	21	-90.711	-137.012	-44.41	0.00035
per cent of ameboid form	group I	3 vs 7	-46.1451	-52.363	-41.212	0.00024
per cent of ameboid form	group I	7 vs 14	-12.34998	-15.3394	-4.7606	0.0005
per cent of ameboid form	group I	14 vs 21	26.8	21.5106	32.0894	0.00007
per cent of ameboid form	group II	3 vs 7	-40.10544	-44.7525	-34.1736	0.00005
per cent of ameboid form	group II	7 vs 14	-16.73206	-24.019	-14.0451	0.00006
per cent of ameboid form	group II	14 vs 21	22.4527	17.1633	27.7421	0.00005
per cent of ameboid form	group I vs group II	7	-6.6821	-11.9715	-1.3926	0.014866
per cent of ameboid form	group I vs group II	21	-6.6473	-12.2228	-1.0717	0.020916

In both groups there were increases of per cent of ameboid form of OX42-ir microglia between the 3rd and 7th and between 7th and 14th and then decreases between the 14th and 21st days of observation (Fig. 5, Tab. III). There were also found the differences of per cent of ameboid form of OX42-ir microglia between groups I and II on the 7th and 21st survival days (Fig. 5, Tab. III).

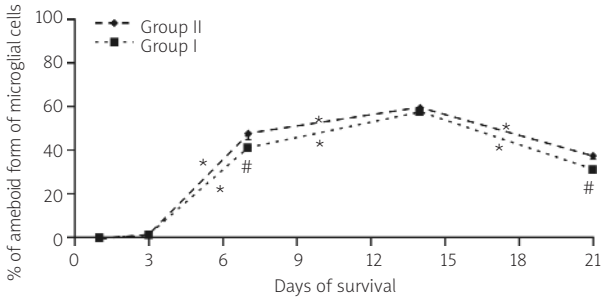

Fig. 5. Per cent of the activated form of OX42-ir cells within the reference area 1, 3, 7, 14 and 21 days after haematoma occurrence in groups I and II. Data are presented as mean±standard error. Significant differences between survival groups are marked by asterisks while between groups I and II -by hashes

Discussion

In the pathology developing in cases of ICH, a prominent role is played by astroglial and microglial cells. We have studied the effect of propofol on the reactivity of astroglia and microglia in the course of experimental ICH. Applying an experimental model is similar to the real condition of the intracerebral haematoma formation. In animals anaesthetized with the use of propofol, an increased and extended activation of both GFAP-IR astrocytes and OX42-IR glia was found.

The clinical study suggests that delayed brain edema (in the 2nd and 3rd weeks after the onset of ICH) is due to a breakdown of hemoglobin induced impairment of the blood-brain barrier [11]. However, Zazulia et al. [40] have proposed other, more speculatively pathophysiological clarification for this late edema formation. From 1 to 14 weeks after ICH, new vessels around haematoma were created. These vessels are devoid of a fully developed blood-brain barrier. Moreover, animal models demonstrated that propofol decreases both cerebral blood flow and cerebral metabolic rate for oxygen [16,24,34]. Some of the animal investigations have suggested that the decrease in cerebral blood flow is greater than the decrease in cerebral metabolic rate for oxygen, that may lead to a critical drop of cerebral perfusion pressure [2,34]. Several clinical studies found a frequent incidence of jugular bulb oxygen saturation values compatible with global cerebral hypoperfusion in patients operated on brain tumors in anaesthesia with the use of propofol [12,19]. Especially, the defective blood-brain barrier may be particularly sensitive to ischemic injury evoked by propofol. This may in part explain our findings.

It may be presumed that astroglial and microglial activations have no direct connection with the injury evoked by intracerebral haemorrhage. Lipid emulsion used as a carrier for propofol may be responsible for glial activation in our investigation. Weight et al. [32] demonstrated that lipid emulsions activated N-methyl-D-aspartate (NMDA) receptors channel. Lipid mediators potentiate NMDA receptor activity [29]. Up-regulation of microglial cell throughout the brain after an intravenous injection of lipopolysaccharide (LPS) was observed by Buttini et al. [4] and Xu et al. [38]. Moreover, LPS released from the outer membrane of Gram-negative bacteria during sepsis may also lead to activation of microglial cells [25].

Propofol evokes a neuroprotective effect, which is apparently mediated by restoration of the glutamate uptake by astrocytes impaired during injury [35]. On the other hand, lipid emulsion stimulates NMDA receptors, that leads to injury. This speculative theory may in part explain our findings especially when we take into account the fact that in some experiments pure substance of propofol (without lipid carrier) was used [35].

In sum, these findings provide evidence for activation of astroglial and microglial cells by propofol. The ability of propofol for modulation of the inflammatory reaction may have a clinical implication. Activation of glial cells in the central nervous system plays a key role during injury and neurodegeneration. Therefore elucidation of the molecular mechanism of our outcome may have a crucial meaning for basic and clinical neurological research.

Acknowledgements

The technical assistance of Mrs. Sylwia Scisłowska is greatly appreciated.

This research was supported by the fund from the Polish State Committee of Scientific Research, grant No 4 PO5A 007 18

References

1. Ardizzone TD, Lu A, Wagner KR, Tang Y, Ran R, Sharp FR. Glutamate receptor blockade attenuates glucose

hypermatabolism in perihematomal brain after experimental intracerebral hemorrhage in rat. Stroke 2004; 35: 2587-2591.
2. Artru AA, Shapira Y, Bowdle T. Electroencephalogram, cerebral metabolic, and vascular responses to propofol anesthesia in dogs. J Neurosurg Anesth 1992; 4: 99-103.
3. Auer LM, Deinsberger W, Neiderkorn K, Gell G, Kleinert R, Schneider G, Holzer P, Bone G, Mokry M, Korner E, et al. Endoscopic surgery versus medical treatment for spontaneous intracerebral hematoma: a randomized study. J Neurosurg 1989; 70: 530-535.
4. Buttini M, Limonta S, Boddeke HW. Peripheral administration of lipopolysaccharide induces activation of microglial cells in rat brain. Neurochem Int 1996; 29: 25-35
5. Fernandes H, Mendelow A. Spontaneous intracerebral haemorrhage: a surgical dilemma. Br J Neurosurg 1999; 13: 389-394
6. Fernandes HM, Gregson B, Siddique S, Mendelow AD. Surgery in intracerebral hemorrhage. Stroke 2000; 31: 2511-2518.
7. Gong C, Hoff JT, Keep RF. Acute inflammatory reaction following experimental intracerebral hemorrhage in rat. Brain Res 2000; 871: 55-65.
8. Hickenbottom SL, Grotta JC, Strong R, Denner LA, Aronowski J. Nuclear factor-kappa B and cell death after experimental intracerebral hemorrhage in rats. Stroke 1999; 30: 2472-2477.
9. Holmin S, Mathiesen T. Intracerebral administration of interleukin-1beta and induction of inflammation, apoptosis and vasogenic edema. J Neurosurg 2000; 92: 108-120.
10. Hua Y, Xi G, Keep RF, Hoff JT. Complement activation in the brain after experimental intracerebral hemorrhage. J Neurosurg 2000; 92: 1016-1022.
11. Huang F-P, Xi G, Keep RF, Hua Y, Nemoianu A, Hoff JT. Brain edema after experimental intracerebral hemorrhage: role of hemoglobin degradation products. J Neurosurg 2002; 96: 287-293.
12. Jansen GF, van Praagh BH, Kedaria MB, Odoom JA. Jugular bulb oxygen saturation during propofol and isoflurane/nitrous oxide anesthesia in patients undergoing brain tumor surgery. Anesth Analg 1999; 89: 358-363.
13. Keep RF, Xi G, Hua Y, Hoff JT (2005) The deleterious or beneficial effects of different agents in intracerebral hemorrhage. Stroke 36: 1594-1596
14. Koeppen AH, Dickson AC, McEvoy JA. The cellular reactions to experimental intracerebral hemorrhage. J Neurol Sci 1995; 134: 102-112.
15. Kowianski P, Karwacki Z, Dziewiatkowski J, Domaradzka -Pytel B, Ludkiewicz B, Wojcik S, Litwinowicz B, Narkiewicz O, Morys J. Evolution of microglial and astroglial response during experimental intracerebral haemorrhage in the rat. Folia Neuropathol 2003; 41: 123-130.
16. Ludbrook GL, Upton RN, Grant C, Gray EC. Cerebral effects of propofol following bolus administration in sheep. Anaesth Intensive Care 1996; 24: 26-31.
17. Megyeri P, Abraham CS, Temesvari P, Kovacs J, Vas T, Speer CP. Recombinant human tumor necrosis factor alpha constricts pial arterioles and increases blood-brain barrier permeability in newborn piglets. Neurosci Letter 1992; 148: 137-140.
18. Montes JM, Wong JH, Fayad PB, Awad IA. Stereotactic computed tomographic-guided aspiration and thrombolysis of intracerebral hematoma, protocol and preliminary experience. Stroke 2000; 31: 834-840.
19. Munoz HR, Nunez GE, de la Fuente JE, Campos MG. The effect of nitrous oxide on jugular bulb oxygen saturation during remifentanyl plus target-controlled infusion propofol or sevoflurane in patienth with brain tumors. Anesth Analg 2002; 94: 389-392.
20. Nath FP, Kelly PT, Jenkins A, Mendelow AD, Graham DI, Teasdale GM. Effects of experimental intracerebral hemorrhage on blood flow, capillary permeability, and histochemistry. J Neurosurg 1987; 66: 555-562.
21. Nehls DG, Mendelow AD, Graham DI, Sinar EJ, Teasdale GM. Experimental intracerebral hemorrhage: progression of hemodynamic changes after production of a spontaneous mass lesion. Neurosurgery 1988; 23: 439-444.
22. Nimkoff L, Quinn C, Silver P, Sagy M. The effects of intravenous anesthetic agents on intracranial pressure and cerebral perfusion pressure in two feline models of brain edema. J Crit Care 1997; 12: 132-136.
23. Ohwaki K, Yano E, Nagashima H, Hirata M, Nakagomi T, Tamura A. Blood pressure management in acute intracerebral hemorrhage. Relationship between blood pressure and hematoma enlargement. Stroke 2004; 35: 1364-1367.
24. Oshima T, Karasawa F, Satoh T. Effects of propofol on cerebral blood flow and the metabolic rate of oxygen in humans. Acta Anaesthesiol Scand 2002; 40: 831-835
25. Pocock JM, Liddle A. Microglial signalling cascades in neurodegenerative disease. In: Castellano-Lopez B, Nieto-Sampedro M. (ed) Glial cell function. Elsevier Amsterdam, London, New York, Oxford, Paris, Shanon, Tokyo 2001; pp. 555-565.
26. Sagara Y, Hendler S, Khoh-Reiter S, Gillenwater G, Carlo D, Schubert D, Chang J. Propofol hemisuccinate protects neuronal cells from oxidative injury. J Neurochem 1999; 73: 2524-2530.
27. Silva Y, Leira R, Tejada J, Lainez JM, Castillo J, Davalos A; Stroke Project, Cerebrovascular Diseases Group of the Spanish Neurological Society. Molecular signatures of vascular injury are associated with early growth of intracerebral hemorrhage. Stroke 2005; 36: 86-91.
28. Stence N, Waite M, Dailey ME. Dynamic of microglial activation a confocal time-lapse analysis in hipocampal slices. Glia 2001; 33: 256–266
29. Tabuchi S, Kume K, Aihara M, Ishii S, Mishina M. Lipid mediators modulate NMDA receptor currents in xenopus oocyte expression system. Neurosci Lett 1997; 237:13-16
30. Tobias JD. Propofol: effects on the central nervous system. J Int Care Med 2000; 15 (5): 237-245.
31. Wagner KR, Xi G, Hua Y, Kleinholz M, de Courten-Myers GM, Myers RE, Broderick JP, Brott TG. Lobar intracerebral hemorrhage model in pigs. Rapid edema development in perihematomal white matter. Stroke 1996; 27: 490-497
32. Weigt HU, Georgieff M, Beyer C, Fohr KJ. Activation of neuronal N-methyl-D-aspartate receptor channels by lipid emulsions. Anesth Analg 2002; 94 (2): 331-337.

33. Werner C, Hoffman WE, Kochs E, Schulte am Esch J, Albrecht RF. The effects of propofol on cerebral and spinal cord blood flow. Anesth Analg 1993 76: 971-976.
34. van Hemelrijck J, Fitch W, Mattheussen M, van Aken H, Plets C, Lauwers T. Effect of propofol on cerebral circulation and autoregulation in the baboon. Anaesth Int Care 1996; 24: 26-31.
35. Velly LJ, Guillet BA, Masmejean FM, Nieoullon AL, Bruder NJ, Gouin FM, Pisano PM. Neuroprotective effects of propofol in a model of ischemic cortical cell cultures. Anesthesiology 2003; 99: 368-375
36. Xi G, Hua Y, Keep RF, Younger JG, Hoff JT. Systemic complement depletion diminishes perihematomal brain edema in rats. Stroke 2001; 32: 162-168.
37. Xi G, Hua Y, Bhasin RR, Ennis SR, Keep RF, Hoff JT. Mechanisms of edema formation after intracerebral hemorrhage: effects of extravasated red blood cells on blood flow and blood-brain barrier integrity. Stroke 2001; 32 : 2932-2938.
38. Xu J, Ling EA. Upregulation and induction of surface antigen with special reference to MHC class II expression in microglia in postnatal rat brain following intravenous or intraperiteneal injection of lipopolysaccharide. J Anat 1994; 184: 285-296.
39. Young Y, Menon DK, Tisavipat N, Matta BF, Jones J. Propofol neuroprotection in a rat model of ischemia reperfusion injury. Eur J Anaesthesiol 2001; 14 (3): 320-326.
40. Zazulia AR, Diringer MN, Derdeyn CP, Powers WJ. Progression of mass effect after intracerebral hemorrhage. Stroke 1999; 30: 1167-1173.